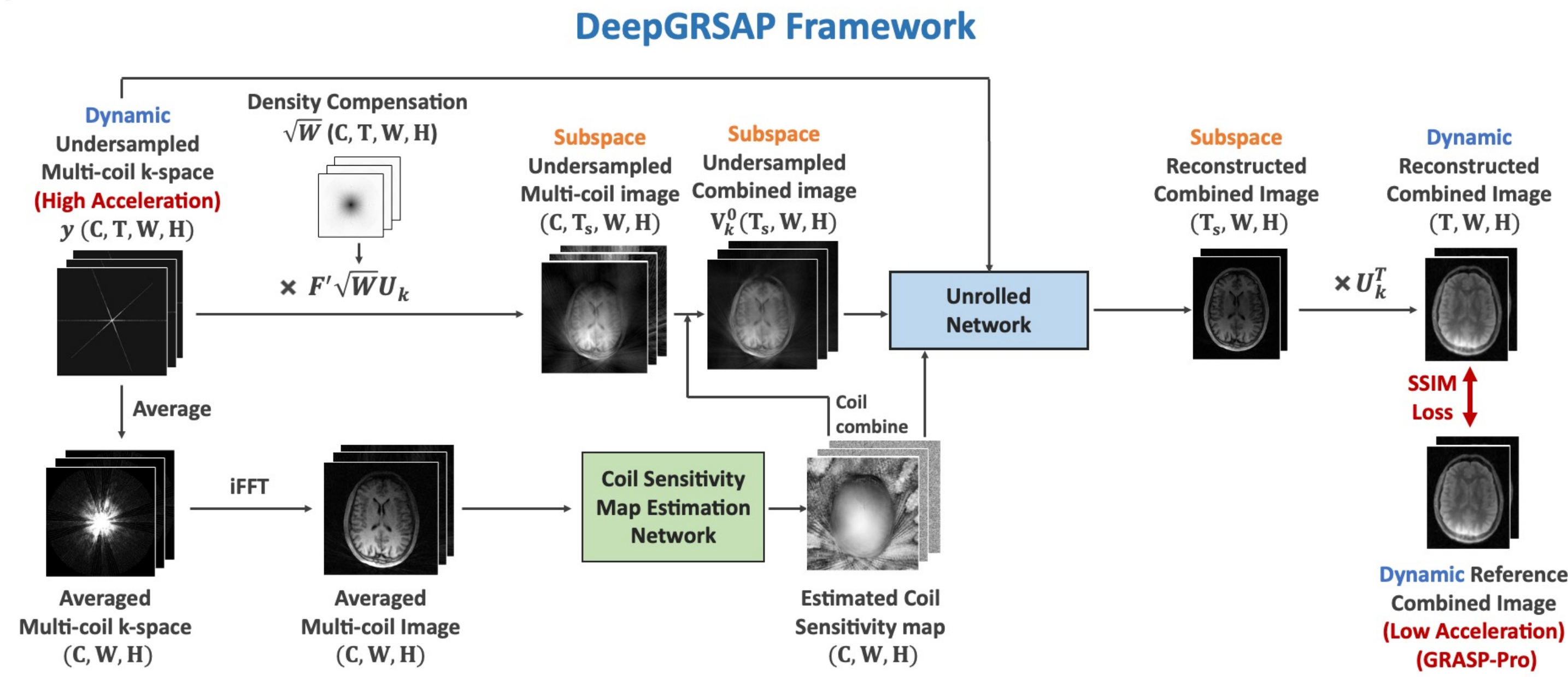


INTRODUCTION

- Golden-angle RAdial Sparse Parallel (GRASP) MRI is a fast-imaging technique that can be applied for accelerated free-breathing dynamic imaging¹. GRASP combines stack-of-stars golden-angle radial sampling with multicoil compressed sensing reconstruction, and it has later incorporated a more advanced low-rank subspace model for further improved imaging performance², called GRASP-Pro.
- However, GRASP-Pro using constrained iterative reconstruction is very slow and does not perform well on a higher acceleration, which represents a major barrier to translate fast MRI techniques for clinical use. In this study, we introduce DeepGRASP, a deep learning-based variant of GRASP. Further experiments on brain 3D T1 mapping, liver 3D T1 mapping and dynamic liver image reconstruction demonstrate that DeepGRASP enables faster reconstruction speed and higher reconstruction quality compared to the conventional framework.

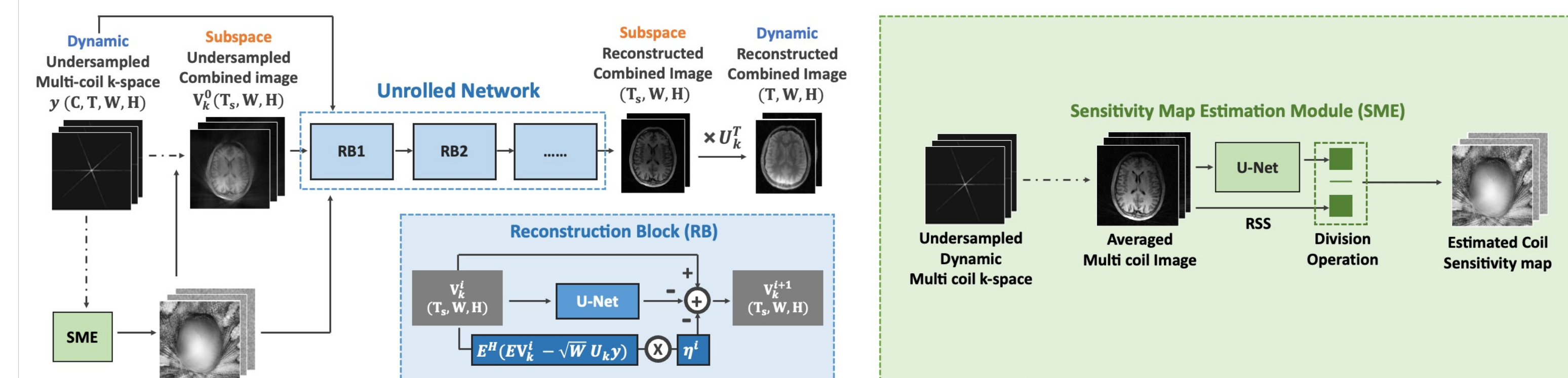
METHODS

DeepGRASP Framework



- The overall training pipeline for DeepGRASP is shown in above Fig. Reference reconstructed images and T1 maps generated from GRASP-Pro with lower accelerations are used as the reference for training. Unlike many deep learning-based MRI reconstruction studies that use fully sampled reference for network training, we use results from undersampled images following iterative reconstruction which is shown to ensure sufficient image quality in a prior study.
- The unrolled network was employed to reconstruct the undersampled dynamic multi-coil k-space data. Similar to the GRASP-Pro reconstruction approach², a low-rank subspace constraint was incorporated during the reconstruction process and the unrolled network only reconstruct subspace images instead of handling the large matrix size of the input image with many dynamic frames. For multi-coil image reconstruction, a coil sensitivity map estimation network was built to estimate the coil sensitivity maps from the averaged multi-coil k-space generated by averaging the undersampled dynamic multi-coil k-space along the time dimension. The estimated coil sensitivity maps were then utilized in the reconstruction process within the unrolled network. Both the unrolled network and the coil sensitivity map estimation network were trained jointly to optimize their performance by enforcing a single SSIM Loss function between reconstructed and reference dynamic images.

Network Architecture



the reconstruction problem can be formulated as the following equation:

$$V_k = \operatorname{argmin}_{V_k} \frac{1}{2} \|EV_k - \sqrt{W}U_k y\|_2^2 + \lambda \Psi(V_k)$$

Where $E = \sqrt{W}U_k M U_k^T F C$ is the encoding operator incorporating coil sensitivities (C) calculated at this resolution, Fourier transform (F), and the GROG³ weighting function (W) for compensating varying sampling density, and M is the sampling mask for the k-space.

y is the sorted full-resolution dynamic k-space shifted to a Cartesian grid using GROG³ and U_k is the pre-estimated basis with K PCs (Principle components).

V_k is the coefficients in subspace to represent the image-series under U_k .

If this formula can be optimized, we are able to recover the V_k and thus reconstruct image-series using the basis U_k .

It can be solved by iterative gradient descent methods. In the i -th step, the image is updated from V_k^i to V_k^{i+1} using:

$$V_k^{i+1} = V_k^i - \eta^i (E^H (E V_k^i - \sqrt{W} U_k y) - \lambda \nabla \Psi(V_k^i))$$

Where η^i is the learning rate, $\nabla \Psi(V_k^i)$ is the gradient of Ψ with respect to V_k^i , and E^H is the hermitian of the forward encoding operator E .

According to above equation, we built upon the unrolled network as shown in the Fig.2, which consists of multiple blocks, each modeled after a single gradient update step. Thus, the i -th block of the unrolled network takes V_k^i as input and computes V_k^{i+1} using:

$$V_k^{i+1} = V_k^i - \eta^i E^H (E V_k^i - \sqrt{W} U_k y) - \operatorname{CNN}(V_k^i)$$

where CNN is a small U-Net that maps complex-valued V_k^i to complex-valued $\lambda \nabla \Psi(V_k^i)$ of the same shape. The η^i as well as the parameters of the U-Net are learned from data.

Evaluation

The framework was evaluated on brain Look-Locker inversion recovery MRI T1 mapping, liver T1 mapping via water/fat separation, and dynamic liver MRI reconstruction.

- For brain T1 mapping, the undersampled image series was reconstructed using DeepGRASP, and another spatiotemporal mapping network was trained to transform the reconstructed images into T1 maps.
- For liver T1 mapping, the undersampled image series with multiple TEs was reconstructed using DeepGRASP. A spatiotemporal water/fat separation network and a T1 fitting network were trained to convert the reconstructed images into T1 maps.
- For dynamic liver MRI reconstruction, a temporal TV constraint was incorporated into the SSIM loss to enhance network optimization.

RESULTS

Brain 3D T1 Mapping

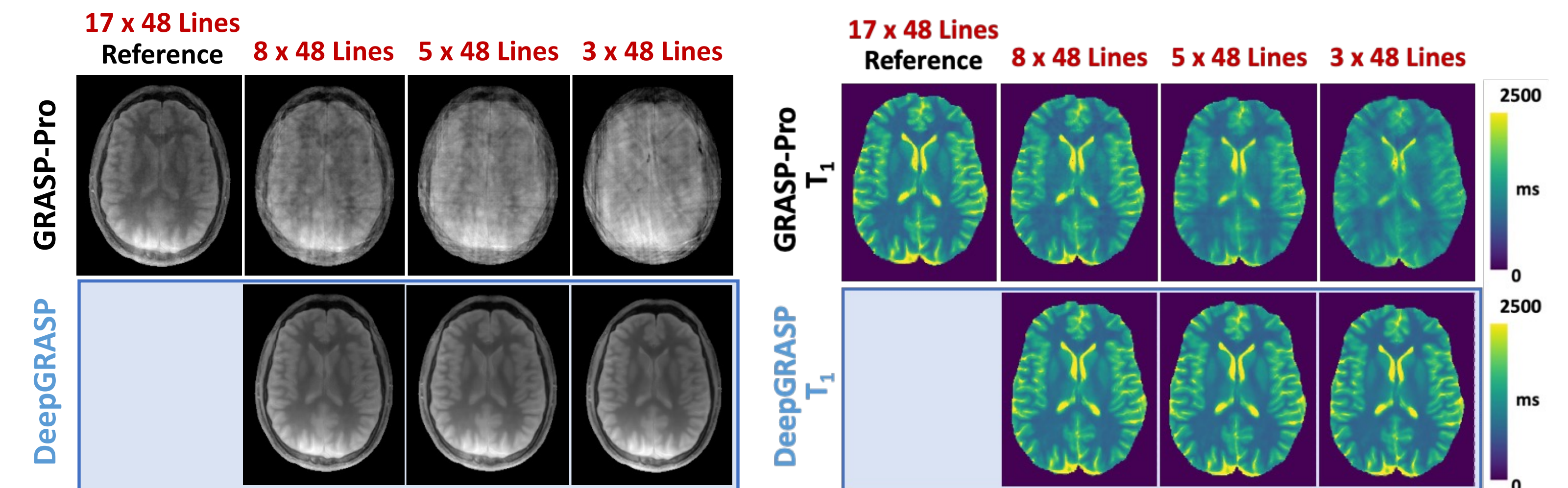


Fig. 3: A representative case comparing one frame of the reconstructed dynamic brain images for T1 mapping and T1 maps from DeepGRASP and GRASP-Pro for brain T1 mapping with 8x48, 5x48 and 3x48 lines.

Liver 3D T1 Mapping with Fat/water Separation

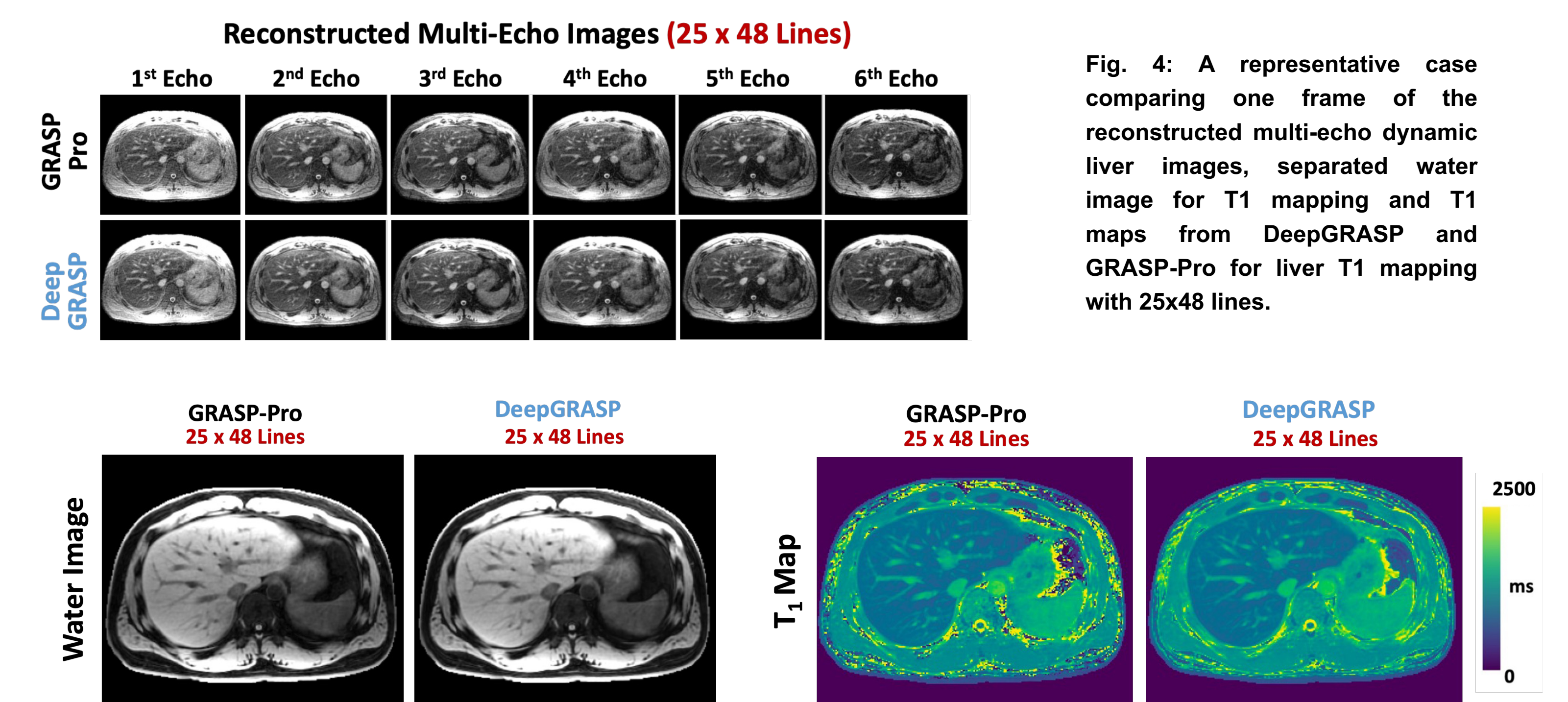


Fig. 4: A representative case comparing one frame of the reconstructed multi-echo dynamic liver images, separated water image for T1 mapping and T1 maps from DeepGRASP and GRASP-Pro for liver T1 mapping with 25x48 lines.

Dynamic Liver Reconstruction

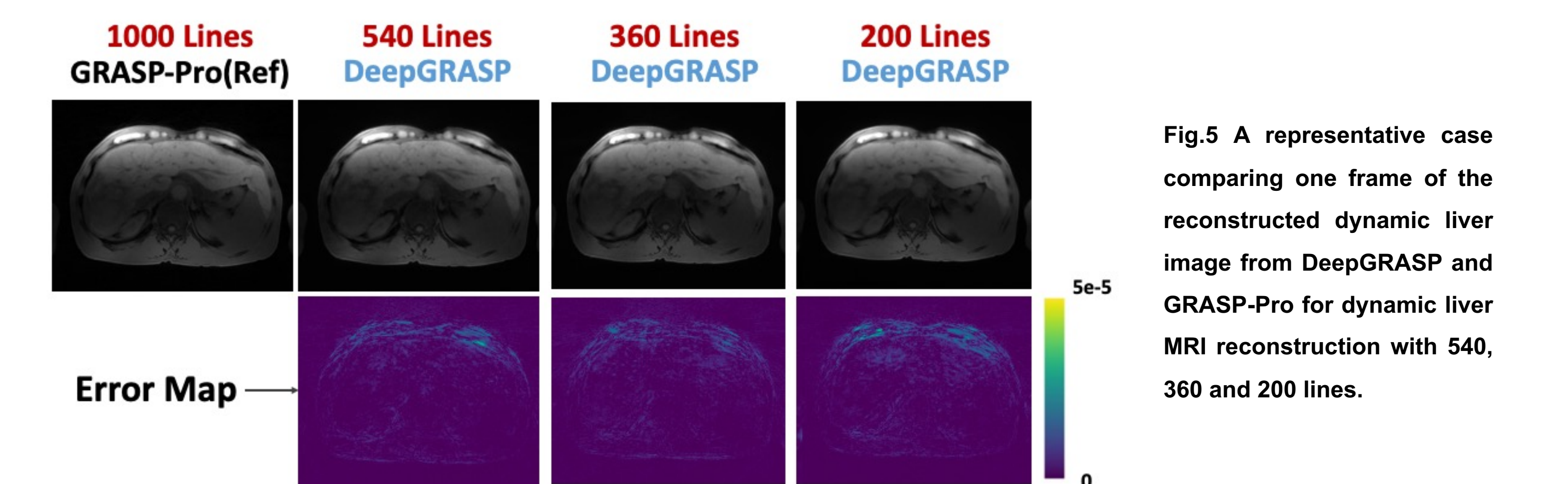


Fig.5 A representative case comparing one frame of the reconstructed dynamic liver image from DeepGRASP and GRASP-Pro for dynamic liver MRI reconstruction with 540, 360 and 200 lines.

DISCUSSION & CONCLUSION

This work proposes DeepGRASP, a deep learning framework for fast and efficient 4D MRI reconstruction based on the GRASP-Pro method. In contrast to the slow and cumbersome standard GRASP, DeepGRASP significantly accelerates 4D MRI reconstruction speed to milliseconds per slice while preserving reconstruction accuracy, which holds great potential for clinical translation.

REFERENCES

- Feng L et al. MRM. 2021;86:97–114;
- Feng L MRMed. 2020;83:94–108;
- Benkert, Thomas, et al. MRM. 80.1 (2018): 286-293.

Grant support: NIH R01EB030549, R21EB032917, R21EB031185, R01AR079442, and R01AR081344